ChemPubSoc Europe

DOI: 10.1002/ejic.201900042

EurJIC European Journal of Inorganic Chemistry

Full Paper

Thiourea Ligands

A Mixed Ligand Platinum(II) Complex: Spectral Analysis, Crystal Structure, Steric Demand of the Ligand, and Bioactivity of *cis*-[Pt(PPh$_3$)$_2$(L^1-*O,S*)]PF$_6$ (L^1-*O,S* = *N,N*-Morpholine-*N*′-benzoyl-thiourea)

Hiram Pérez,*[a] Raúl Ramos,[b] Ana M. Plutín,*[b] Raúl Mocelo,[b] Mauricio F. Erben,[c] Eduardo E. Castellano,[d] and Alzir A. Batista*[e]

Abstract: A novel mixed platinum(II) complex with general formula [Pt(PPh$_3$)$_2$(L^1-*O,S*)]PF$_6$ has been synthetized and characterized by elemental analysis, molar conductivity, and by IR and NMR (^{1}H, ^{13}C and ^{31}P) spectroscopic methods. The crystal structure has been determined by single-crystal X-ray crystallography. The molecule presents an almost ideal square-planar geometry, and the crystal is stabilized by weak C–H···O and C–H···F hydrogen bonds, and C–H···π stacking interactions. The steric congestion of ligands is described by "exact" cone and solid cone angles, and the percentage of metal surface shielded by the ligands. The results are compared to closely related palladium complexes. The X-ray structure revealed the proximity of the *ortho* phenyl proton of one PPh$_3$ ligand to platinum(II) showing rare intramolecular C–H···Pt anagostic binding interaction. The title complex was determined to be active against tumor cells, and it also showed a moderate inhibitory action against *mycobacterium tuberculosis*.

1. Introduction

N-alkyl/aryl- (H$_2$L) and *N,N*-di(alkyl/aryl)-*N*′-benzoylthiourea (HL) have attracted interest in view of their selective co-ordination towards transition metals, and particularly the platinum group metals, leading to a wide range of bioactivity,[1–3] including cytotoxic activity against cancer, including leukemia and solid tumors.[4–5] These properties have also been observed in metal complexes with acylthiourea derivatives.[6–9] Furthermore, the acylthioureas are characterized for altering electronic and steric effects in its metal complexes, which have made possible the design of effective industrial catalysts.[10–12]

On the other hand, it is well known that the phosphines have many applications in organometallic chemistry, specifically as ligands in homogeneous catalysts,[13] and it has curiously been reported that Ru^{II}, Ru^{III}, Co^{III} and Cu^{I} complexes containing *N*-di(alkyl/aryl)thiourea together with triphenylphosphine present catalytic activity for the oxidation of alcohols.[12] In the triphenylphosphine-containing complexes, the conformation of the phenyl rings often contributes to the bulkiness of the complex, which is interesting because the bulkiest part of the molecule generally determines its shape and reactivity.[14]

There are in the literature suggestion that the addition of the triphenylphosphine the hydrophobicity of the complexes increase, resulting in more cytotoxic activities, probably due the increasing of drug uptake.[15–16] Indeed, ruthenium(II) arene complexes containing the triphenylphosphine as ligand displayed IC$_{50}$ values lower than those found for cisplatin toward some cancer cells.[16–17]

The influence of steric effects of a ligand on the structures and reaction rates of organometallic and coordination compounds has been discussed in the literature using Tolman's cone angle (θ).[18] Taking into account the inaccuracy of several empirical parameters that were assumed by Tolman, X-ray crystal structure data have been used as a basis for estimating ligand cone angles of phosphine ligands from the atomic coordinates observed in the crystal structures of transition metal phosphine compounds.[19]

Recently, the "exact" cone angle (θ°) has been presented as a new ligand steric descriptor based on the idea of covering the ligand in the most acute possible cone, being also useful for determining the cone angle of any ligand, particularly for environments with free rotation.[20] An interesting cone angle history can be found in literature, which offers a detailed expla-

[a] *Departamento de Química General e Inorgánica, Universidad de La Habana, 10400, La Habana, Cuba*
[b] *Laboratorio de Síntesis Orgánica, Facultad de Química, Universidad de La Habana, 10400, La Habana, Cuba*
E-mail: anap@fq.uh.cu
[c] *CEQUINOR (UNLP-CONICET, CCT La Plata), Departamento de Química, Facultad de Ciencias Exactas, Universidad Nacional de La Plata, Bv. 120 1465, La Plata, 1900, Argentina*
[d] *Instituto de Física de São Carlos, Universidade de São Paulo, 05508-090 São Carlos-SP, Brazil*
[e] *Departamento de Química, Universidade Federal de São Carlos, 13565-905 São Carlos-SP, Brazil*
ORCID(s) from the author(s) for this article is/are available on the WWW under https://doi.org/10.1002/ejic.201900042.

nation on the need to develop a method for computing the cone angle in any situation.[21]

Other descriptors used for quantifying steric demand are the solid cone angle (Θ) and solid angle (Ω),[19b] the former derived from the area filled by the ligands on the surface of a sphere centered at the metal atom, and the latest associated to the shadow cone of a ligand supposedly illuminated from the metal center. The "exact" solid cone angle ($\Theta°$) of ligand[21–22] cannot be modeled using the cone angle model, and it is especially useful in the case of multidentate ligands rotationally hindered. The solid angle (Ω) can be calculated to quantify the total steric shielding through the so-called G-parameters.[23] Thus, the G(L) and G(M) parameters describe the ligand and metal surface shielding, respectively, as a percentage of the maximum solid angle (4π steradians), whereas G(complex) parameter gives the G value for the entire complex, all ligands treated as one.

In this work we report the synthesis, spectroscopic properties, crystal structure and biological activity of *cis*-[Pt(PPh_3)$_2$-(L^1-*O,S*)]PF_6 complex (***L¹-O,S*** = *N,N*-morpholine-*N'*-benzoylthiourea), focusing our interest in the coordination geometry, the steric demand of both the ligands, and antitumor and antibacterial activity. It is reported that only the crystal structures of the mononuclear complexes Tc^{III}, Re^{III},[24] and Pd^{II},[25] as well as the Rh^{I} dinuclear complex[26] containing triphenylphosphine and benzoylthiourea respectively, so this work can contribute to preclinical studies and the development of new reagents and catalysts to be used in organic synthesis.

2. Results and Discussion

2.1. IR Spectra

Infrared spectra suggest the formation of the complex by deprotonation of ***L¹-O,S*** free ligand during its coordination to platinum ion. Thus, the typical NH stretching that appears as a wide and strong absorption at 3279 cm^{-1} in the free ligand, disappears after its coordination to the metal (Figure S1). By the other hand, the band ν(CN) at 1481 cm^{-1} in the complex is absent in the free ligand, suggesting the formation of a heterocyclic ring according to Scheme 1. In addition, the band at 1517 cm^{-1} is assigned to C=O group in the complex, and the vibration frequency is decreased when compared to the corresponding band at about 1661 cm^{-1} for the free ligand, in agreement with the literature.[27] The absorption at 878 cm^{-1} in the free ligand is attributed to the ν(C–S) stretching, shifted to the 769 cm^{-1} in the complex. The absorption at 471 cm^{-1} is assigned to the Pt–O vibration mode and the assignment of the Pt–S stretching at about 360 cm^{-1} is in accordance with the literature.[28–31] These results suggest that L^1 ligand is attached to the metal through the oxygen and sulfur atoms in a chelating form. By the other hand. The IR spectrum shows signals associated with the presence of PPh_3 ligand and the PF_6- anion, thus, signals at 3057, ν(C–H) (PPh_3); 842, ν(P–F); 692, νP-Ph (Ph_3–P–Ph_3); 550, ν(Pt–P) cm^{-1} as reported in previous work,[32] suggesting direct coordination of the phosphorus atom to the platinum ion, in agreement with the results of crystal structure determination (Figure S2).

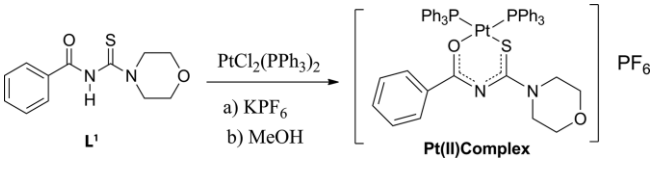

Scheme 1. Synthesis of *cis*-[Pt(PPh_3)$_2$(L^1-*O,S*)]PF_6 (***L¹-O,S*** = *N,N*-morpholine-*N'*-benzoylthiourea).

2.2. ^{1}H NMR, ^{13}C NMR and ^{31}P NMR Spectra

The ^{1}H NMR spectrum of the ***L¹-O,S*** free ligand basically shows three sets of well-separated signals corresponding to the benzene substituents, morpholine ring and the NH proton (Figure S3). The latter appears as a singlet at 8.60 ppm and disappears after coordination to the metal.[33–34] The methylene protons in the morpholine ring appear as two broad triplets at 4.22 and 3.65 ppm, and a multiplet at 3.83 ppm that integrates four protons, because they are attached to the nitrogen atom. All the protons present in the complex appear at higher chemical shifts than in the free ligand. The aromatic protons are visible as a complex pattern in the region 8.13–7.00 ppm as in related compounds.[28] The signals corresponding to the methylene protons in morpholine ring (Figure S4) are observed in form of triplets ranging from 4.22 to 3.65 ppm. ^{13}C NMR spectrum of the L^1 free ligand shows signals at 179.25 and 163.30 ppm which are ascribed to the carbon atoms of C=S and C=O groups, respectively (Figure S6). However, the former signal is shifted to higher field by 9.64 ppm, and the latter signal to lower field by 4.49 ppm in the complex (see Figure S7).

^{31}P {^{1}H} NMR spectrum of complex indicates that there are two coordinated triphenylphosphine ligands in *cis* position. The precursor [$PtCl_2(PPh_3)_2$] in CH_2Cl_2 solution shows a singlet peak for phosphorus atoms at 13.72 ppm, whereas the complex shows two doublets at about 20.55 and 9.34 ppm revealing the existence of two magnetically different phosphorus atoms bonded to platinum(II) ion. A multiple signal of the PF_6^- anion appears in the region 138–158 ppm (Figures S8 and S9) as in similar complexes previously reported.[35] The molar conductivity shows that the complex is a cationic species.[36]

2.3. X-ray Structure

The ORTEP diagram of title complex is shown in Figure 1 with atom numbering scheme Selected bond lengths, bond angles and torsion angles are summarized in Table S1 (Supporting Information). The platinum(II) ion is coordinated by two phosphorus atoms of two bulky triphenylphosphine ligands, and the oxygen and sulfur atoms of one bidentate L^1 ligand forming a four-coordinate *cis*-planar geometry as occurs in the structural chemistry of bis-chelates benzoylthioureas with d^8 or d^9 ions.[37] A PF_6^- group acts as outer-sphere anion of the complex. The τ_4 index has been proposed to describe the geometry of four-coordinate complexes, with values falling between 1.00 for a perfect tetrahedral geometry and zero for an ideal square-planar geometry.[38] The τ_4 index calculated for title complex is equal to 0.06 indicating an almost perfect square planar envi-

ronment around the Pt^{II} ion. The Pt–O [2.061(4) Å], Pt–S [2.308(2) Å] and Pt–P [average 2.277(1) Å] bond lengths are comparable to those observed in similar complexes.[39,40] The lengths of C–O, C–S and C–N bonds in the chelate ring are between characteristic single and double bond lengths as result of the existence of electronic delocalization.

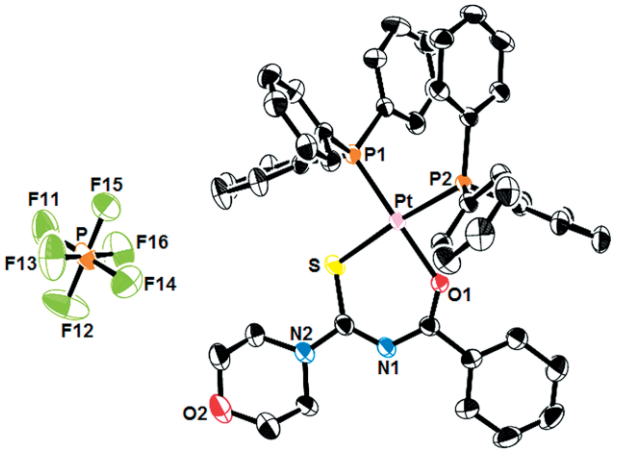

Figure 1. ORTEP diagram of the title complex with heteroatom numbering scheme and ellipsoids at 30 % probability level; H-atoms are omitted for clarity.

A clearly puckered system is observed for the six-membered morpholine ring. The q(3) puckering amplitude value (–0.5524 Å) is very longer than the corresponding q(2) amplitude value (0.0580 Å), which is very close to zero. The q(3) value is also very similar to the total puckering amplitude QT = 0.555 Å, which lies slightly under the QT value of 0.63Å for ideal cyclohexane chair.[41] These results indicate that the morpholine ring adopts a slightly distorted chair conformation. The crystal packing (Figure 2) reveals that the complex is stabilized by weak C–H···O hydrogen bonds forming dimers $R_2^2(8)$, weak C–H···F hydrogen bonds involving four fluorine atoms of the PF_6^- anion, and a significant intermolecular C–H···π interaction (H125···*Cg*4 = 2.66 Å, *Cg*4 = centroid of C111–C116 ring)[42] involving phenyl rings. Geometry of intermolecular interactions is shown in Table S2 (Supporting Information).

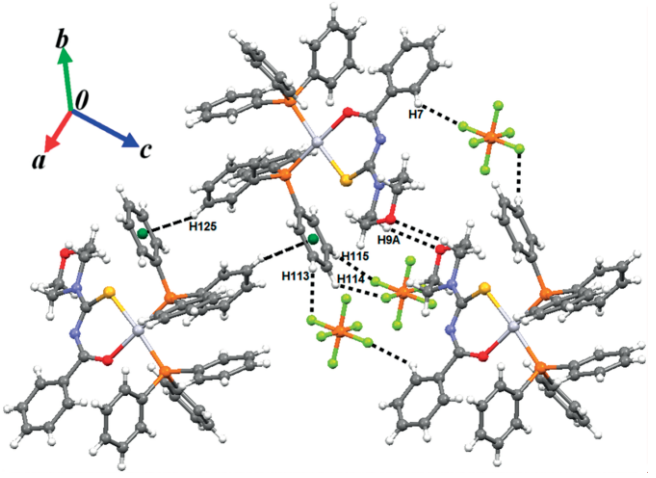

Figure 2. View of crystal packing for title complex. Hydrogen bonds and C–H···π contacts are shown as dashed lines. *Symmetry codes*: (i) –*x*, 1 – *y*, 1 – *z*; (ii) 1 – *x*, 1 – *y*, –*z*.

2.3.1. Steric Description of the Ligands

In order to measure the steric demand of ligands, the "exact" cone (θ°) angles of the two M – PPh_3 (M = metal) fragments for title complex (hereafter **1**) were calculated and compared with five closely related Pd^{II} complexes editorial query: the CSD Refcode are given in Table 1[25]. The results listed in Table 1 show longer exact cone angle values than that the idealized Tolman standard value of 148°[18] for all structures in agreement to the literature,[20] with similar mean absolute deviations of 17.6 and 17.9°, respectively. The higher cone angle value of one PPh_3 ligand for **1** (θ° = 171.9°) is slightly longer than the corresponding average value of 169.0° for Pd complexes, supporting the fact that in general as the actual M–P distance increases (from 2.241/2.314 Å for Pt to average 2.258/2.346 Å for Pd), the cone angle should decrease.[20] Unlike YIXRUU, the remaining complexes appear bonded by two PPh_3 ligands (Table 1) showing remarkable internal mismatches of 12.7° and (4–9°) in their cone angles for Pt and Pd complexes, respectively. The observed differences reveal the significant effect of the chemical environment on the steric bulk of a ligand.

Table 1. Exact cone θ° angle of M–PPh_3 (M = metal) fragment, exact solid cone Θ° angle of M–Th fragment, and G-parameters[a] for **1** and palladium related complexes.

Complex	Formula[b]	θ^0 [deg] M–PPh_3	Θ°[deg] M–Th	G-parameters [%] Complex	Metal
1	$[Pt(PPh_3)_2(L^1\text{-}O,S)]\cdot PF_6$	171.9	139.6	81.1	68.2
		159.2	–	–	–
YIXRUU	$[PdCl(PPh_3)(L^2\text{-}O,S)]$	158.5	141.4	70.7	65.2
YIXROO	$[Pd(PPh_3)_2(L^3\text{-}O,S)]\cdot PF_6$	164.7	144.1	83.0	67.6
		169.5	–	–	–
YIXSOP	$[Pd(PPh_3)_2(L^4\text{-}O,S)]\cdot PF_6$	163.4	146.2	83.3	67.2
		169.3	–	–	–
YIXREE	$[Pd(PPh_3)_2(L^5\text{-}O,S)]\cdot PF_6$	178.3	141.4	81.3	68.0
		154.9	–	–	–
YIXRII	$[Pd(PPh_3)_2(L^6\text{-}O,S)]$	169.6	143.5	82.9	67.4
		165.1	–	–	–

[a] G(complex) = The G value for the complex, all ligands treated as one; G(metal) = percentage of metal surface shielded by the ligated atoms only. [b] ***L*¹-*O,S*** = *N,N*-morpholine-***N′***-benzoylthiourea; ***L*²-*O,S*** = *N,N*-dimethyl-***N′***-benzoylthiourea; ***L*³-*O,S*** = *N,N*-diphenyl-***N′***-benzoylthiourea; ***L*⁴-*O,S*** = *N,N*-dibenzyl-***N′***-benzoylthiourea; ***L*⁵-*O,S*** = *N,N*-diethyl-***N′***-furoylthiourea; HL^6 = *N,N*-diphenyl-***N′***-furoylthiourea.

Table 2. IC_{50} values of complex **1**, precursor complex, ethambutol, cisplatin and ligand ***L¹-O,S*** in cell lines (L929, MDA-MB 231, and DU-145) after 48 hours of incubation, selective index (SI) and MIC values of anti-mycobacterial activity.

IC_{50} (μmol L^{-1}) Compound	DU-145	MDA-MB-231	L929	SI[a]	SI[b]	MIC μg/mL	μmol/L
1	3.09 ± 1.1	6.92 ± 0.60	> 100	> 32.36	> 14.45	> 25	> 22.40
$[PtCl_2(PPh_3)_2]$	> 100	> 100	16.53 ± 2.3	–	–	> 25	> 47.32
Ethambutol	–	–	–	–	–	1.02	5.62
Cisplatin	2.00 ± 0.20	2.43 ± 0.20	> 100	> 8.26	> 6.80	–	–
L^1	> 100	> 100	> 100	–	–	> 25	> 25

[a] IC_{50}L929/IC_{50}DU-145. [b] IC_{50}L929/IC_{50} MDA-MB-231; ***L¹-O,S*** = *N*,*N*-morpholine-*N*′-benzoylthiourea.

To avoid the complications with cone angles for estimating the steric demand of multidentate ligands, and the steric crowding about the metal center when several ligands are present,[22] instead of θ° we have calculated the "exact" solid cone angles Θ° of the bidentate morpholine-thiourea ligand for **1** and the five related palladium complexes (Table 1). The Θ° values vary from 139.6° for **1** to 146.2° for YIXSOP correlating well with the bulk of substituents at the thiourea backbone, as expected. That way, bulkier substituents, higher the solid cone angle. In the series of palladium complexes, the lower Θ° value of 141.4° corresponds to YIXRUU and YIXREE with small dialkyl-thiourea ligands, in comparison to the other three complexes with bulkier diaryl-thiourea ligands. The big diphenyl group enlarges Θ° by 2.1° for YIXRII complex, and a little longer (2.7°) for YIXROO due to the increased size of the benzoyl ring related to the furoyl ring in the former complex. The presence of the bulkiest dibenzyl group is compatible with the maximum enlargement (4.8°) of Θ° for YIXSOP.

In order to evaluate the probability of an incoming reagent not accessing the metal center, the percentages of metal coordination sphere shielded by each ligand [G(L)], the G value for the complex with all ligands treated as one cumulative ligand [G(complex)], and percentage of metal surface shielded only by the ligated atoms [G(M)] were computed from ligand solid angles Ω (Table S3, Supporting Information), using zero energy point radii (r_Z) instead of the van der Waals radii.[23]

A Solid G view for complex **1** is shown in Figure 3 highlighting the areas of the ligands ($2PPh_3$ and L^1) projection shadow onto a sphere of an arbitrary radius. The percentage of the sphere shielded by the thiourea L^1 ligand (32.8 %) is longer than those by the PPh_3 ligands (average 27.1 %), and hence the remaining open area (white) of the sphere where an incoming reagent could bind represents only 13.1 %. The G(complex) value indicate that all the ligands shield 81.1 % of the platinum's coordination sphere, whereas the G(Pt) value of 68.2 % denote that there is only a 31.8 % chance that an incoming reagent reaches the metal center. The G(Pd) values are slightly shorter (67.2–68.0 %) for the four palladium complexes bonded by two PPh_3 ligands (Table 1), and even shorter (65.2 %) for the chloro complex (YIXRUU) as result of its decreased steric crowding about the Pd atom.

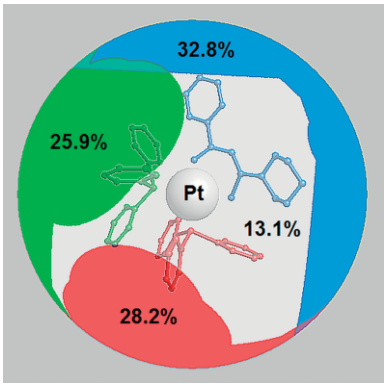

Figure 3. View of projection of L^1 (blue) and PPh_3 (green and gray) ligands in complex **1** onto a sphere of an arbitrary radius of 10 Å. The Pt atom is shown as a large grey sphere of an arbitrary radius for easy visualization.

2.3.2. Anagostic Interactions

The packing effects together with the steric and electronic hindrance of both bulky PPh_3 ligand and diamagnetic d^8 square-planar Pt^{II} allow the aromatic *ortho*-proton H122 of a PPh_3 group to be nearly close to one of the vacant positions around the platinum atom, leading to a rare intramolecular anagostic interaction with Pt···H122= 2.851(1) Å and C122–H···Pt = 123°. Anagostic C–H···M interactions are characterized by relatively long M···H distances (2.3 to 2.9 Å) and large angles (110 to 170°), in comparison to agostic interactions which are characterized by relatively short M–H distances (1.8 to 2.3 Å) and C–H···M angles ranging from 90 to 140°.[43–45] Anagostic interactions are interesting due to possible influences on the mechanism of C–H activation.[46–48]

Furthermore, the effect of the intramolecular Pt···H–C interaction on the donor phosphine ligand has been analyzed by the closely inspection of the infrared spectra in the C–H stretching vibration. This is a crowded region because of the many C–H bonds present in the complex, but a very strong band is observed at 3057 cm^{-1}, which can be assigned to the C–H stretching mode in the phosphine group.[49,50] It is accepted that anagostic interactions is mostly electrostatic in character, in line with the strong C–H absorption observed in the infrared spectrum. Also, the comparison of the proton signals in the ^1H NMR spectra of the ligand and the complex shows that signals due to the benzene ring in the phosphine complex appear at higher fields.

2.4. Biological Activity

The effect of the PPh_3 group in the antitumor activity of Ru^{II} complexes has been studied by Sáez et al. and a noticeable increment of the antitumor activity and cytotoxicity of the complexes was found due to the presence of the PPh_3 ligand.[16]

Similarly, the high cytotoxic activity in vitro of Ru^{II} complexes containing cymene and phosphine ligands reported by was attributed to Ru^{II} species still bearing the phosphorus ligand bounded to the metal center.[17]

The free ligand, the title complex **1** and precursor $[PtCl_2(PPh_3)_2]$ were tested against the tumor cells (L929, MDA-MB 231 and DU-145) and compared with the cytotoxicity of cisplatin as well as evaluated under the same experimental conditions as it appears in Table 2. The IC_{50} value of 16.53 ± 2.38 μmol L^{-1} was calculated from the dose-survival curve generated by the MTT assay obtained after drug treatment. As can be seen, the value of IC_{50} (> 100 μg/mL) for the complex is very high for L929, indicative of selectivity toward tumor cell. The free ligand and the complex were also tested in strains of *mycobacterium tuberculosis* (H37Rv ATCC 27294) using the MABA methodology. The MIC values >25, and 1.02 μg/mL for the free ligand, complex and ethambutol, respectively, are shown in Table 2.

As can be seen from Table 2, the complex **1** in general is more cytotoxic than the precursor, $[PtCl_2(PPh_3)_2]$. This is probably due to the fact the compound is anionic, and more soluble in the biological medium than the $[PtCl_2(PPh_3)_2]$ complex. Worth it to mention that the $[PtCl_2(PPh_3)_2]$ complex is stable in DMSO/H_2O (9:1) solution for at least 96 h, as showed by $^{31}P\{^1H\}$ NMR (Figure S10).

The selective indexes of complex (**1**) for the DU-145 and MDA-MB-231 are much higher than those found the Pd^{II} complexes of *N*,*N*-disubstituted-*N*′-acylthioureas.[25]

According to the data from Table 2, the complex showed a moderate inhibitory action against mycobacterium tuberculosis (H37Rv ATCC 27294) when compared to the reference drug (ethambutol). Also, the observed MIC values suggest that the complex is active against the tumor cells MDA-MB 231 (6.92 ± 0.60) and DU-145 (3.09 ± 1.1), although lower than other platinum(II) and palladium(II) complexes previously obtained by us.[25,50,51]

3. Conclusions

A new ligand mixed Pt^{II} complex with triphenylphosphine and benzoylthiourea, *cis*-$[Pt(PPh_3)_2$ ***L*^{1}*-O,S***$]PF_6$ (**1**), has been synthetized, fully characterized, and its structure determined by X-ray diffraction showing almost perfect square-planar coordination geometry. A rare intramolecular anagostic C–H···Pt interaction is detected, and the crystal packing is stabilized by weak hydrogen bonds and C–H···π interactions. Calculations of steric descriptors for **1** and related Pd^{II} compounds revealed sterically congested complexes. The complex presents cytotoxic and antimycobacterial activity. Information obtained from this work may be useful to initiate pre-clinical studies of title complex, and for the design of new catalysts.

4. Experimental Section

4.1. Materials and measurements

The precursor $[PtCl_2(PPh_3)_2]$ was obtained from Sigma. All reagents were purchased with reagent grade and used without further purification. Solvents were dried and used freshly distilled, unless otherwise specifically indicated. Thin layer chromatography (TLC) was performed on 0.25 mm silica gel pre-coated plastic sheets (40/80mm) (Polygram-SIL G/UV254, Macherey & Nagel, Düren, Germany) using benzene (caution)/methanol (9:1) as eluent. The determination of C/H/N/S was done using a Fisons – EA-1108 CHNS Element Analyzer. The IR spectra were recorded on a FT-IR Bomem-Michelson 102 spectrometer in the 4000–200 cm^{-1} region using KBr pellets. The molar conductivity Λ_m was obtained on a Meter Lab CDM2300 instrument using 1.0 mM solution of complex in dichloromethane. ^1H, $^{31}P\{^1H\}$ and $^{13}C\{^1H\}$ NMR spectra were recorded on a Bruker DRX 400 MHz, internally referenced to TMS, chemical shift (δ), multiplicity (m), spin–spin coupling constant (*J*), integral (I). $CDCl_3$ was used as solvent. The displacement $^{31}P\{^1H\}$ is reported in relation to H_3PO_4 (85 %). NMR experiment with Single Heteronuclear 2D Quantum Coherence (HSQC) was performed in order to unambiguously assign the C=O and C=S signals of the complex.

4.2. Synthesis of *N*,*N*-morpholine-*N*′-benzoylthiourea (L^1)

Intermediate compound *N*,*N*-morpholine-*N*′-benzoylthiourea was synthesized as described previously, and identity of the product was confirmed by comparing their ^1H and $^{13}C\{^1H\}$ NMR data with those reported in literature.[52] Yield: 0.213 g (85 %), Anal. Calcd. for: $[C_{12}H_{14}N_2O_2S]$: C, 57.58; H, 5.64; N, 11.19; S, 12.81 %; found C, 57.00; H, 5.50; N, 10.90; S, 12.00 %. IR (KBr; ν/cm^{-1}): 3279 (N–H), 2980 (C–H), 1661 (C=O), 1603 (C=C), 1520 (band I N–C=S), 1475(C–O–C) 1267 (band II N–C=S), 1114 (band III N–C=S), 932 (band IV N–C=S). ^1H NMR ($CDCl_3$, δ, ppm): 8.60 (^1H, s, NH1, exchange with D_2O), 7.84–7.46 (m, 5H, Ph), 4.22 (t, 2H, CH_2), 3.83 (m, 4H, CH_2), 3.65 (m, 2H, CH_2) ^{13}C NMR ($CDCl_3$, δ, ppm): 179.25 (C=S), 163.30 (C=O), 133.20–127.83(Ph), 66.22 (CH_2-O), 52.55, 51.60 (CH_2-N).

4.3. Synthesis of *cis*-$[Pt(PPh_3)_2(L^1\text{-}O,S)]PF_6$ {*cis*-bis(triphenylphosphine)(*N*,*N*-morpholine-*N*′-benzoylthioureato-k^2*O*,*S*)platinum(II) hexafluorophosphate}

A solution of $[PtCl_2(PPh_3)_2]$ (1.580 g, 2 mmol) in 5 mL of methanol was added dropwise to a solution of ***L*^{1}*-O,S*** (0.50 g, 2 mmol) dissolved in 30 mL of the same solvent, and KPF_6 (0.368 g, 2 mmol) (Scheme 1). The mixture was heated under magnetic stirring at 80 °C for 2 h, and later left overnight into the refrigerator. The white solids obtained were filtered off and washed successively with hot water and hot hexane (3 × 20 mL). Yield: 1.77 g (80 %). Anal. Calcd. for $C_{48}H_{43}F_6N_2O_2P_3PtS$: C, 51.76; H, 3.89; N, 2.51; S, 2.88 %; found C, 52.48; H, 4.30; N, 3.05; S, 2.70 %; m.p. 249–251 °C; Λ_m = 47.6 Ω^{-1} cm^2 mol^{-1}. IR (KBr; ν/cm^{-1}): 3057, ν(CHPPh$_3$); 1585 ν(C=N); 1497, ν(C=O); 842, ν(P–F); 743, ν(C=S); 692, ν(Ph$_3$–P–Ph$_3$); 550, ν(Pt–P). ^1H NMR (400MHz, $CDCl_3$): δ (ppm) = 8.12–7.00 (30 H-atoms of PPh_3, 5 H-atoms of Ph), 4.19 (t, 2H, CH_2), 3.78 (t, 2H, CH_2), 3.68 (bs, 4H, CH_2); $^{13}C\{^1H\}$ NMR (100 MHz, $CDCl_3$): δ (ppm) = 169.61 (C=S), 167.79 (C=O), 134.55, 134.44, (d, C_{meta}-PPh_3, $3J_{C-P}$10.63, 10.48 Hz), 132.31, 131.85 (C_{para}-PPh_3), 132.23, 131.85, (C_{para}-Ph), 129.77 (C_{meta}-Ph), 128.97, 128.86, (d, C_{ortho}-PPh_3, $^2J_{C-P}$12.26, 11.60 Hz), 127.85 (C_{ortho}-Ph), 127.21, 126.63, (d, $C_{quaternary}$-PPh_3, $^1J_{C-P}$ 66.90, 57.59 Hz), 66.36 and 53.44 ($2CH_2$), 49.45 and 47.58 ($2CH_2$). $^{31}P\{^1H\}$ NMR (161.98 MHz, CH_2Cl_2): δ (ppm) = 21.03, 8.78 (d), $^2J_{P\text{-}P}$ = 24.29 Hz, 29.95 (d); 10.73 (d); $^2J_{Pt\text{-}P}$ = 31.22 Hz, 21.16 (d); –2.60 (d); $^2J_{Pt\text{-}P}$ = 38.53, Hz –144.51, (m, PF_6^-).

4.4. X-ray crystallography

A suitable single crystal was obtained by slow evaporation of $CHCl_3$:*n*-hexane (3:1) solution of the complex. Diffraction data were collected on an Enraf-Nonius Kappa-CCD diffractometer with graphite-monochromated Mo-K_α radiation (λ = 0.71073 Å) at 293(2) K. The final unit cell parameters were based on all reflections. Data

Table 3. Crystal data and structure refinement for title complex.

Empirical formula	$C_{48}H_{43}F_6N_2O_2P_3PtS$
Formula weight	1113.90
Temperature /K	293(2)
Crystal system	*Triclinic*
Space group	$P\bar{1}$
Unit cell dimensions	a = 11.4855(6) Å
	b = 14.8935(7) Å
	c = 14.9173(6) Å
	α = 115.550(3)°
	β = 91.469(3)°
	γ = 90.729(3)°
Volume /Å^3	2300.65(19)
Z	2
ρ calcd. /mg mm^{-3}	1.608
μ /mm^{-1}	3.265
F(000)	1108
Crystal size /mm^3	0.313 × 0.127 × 0.03
Theta range for data collection	2.56 to 26.00°
Index ranges	$-14 \le h \le 14$
	$-18 \le k \le 16$
	$-18 \le l \le 18$
Reflections collected	25830
Independent reflections	9018 [R(int) = 0.0610]
Data/restraints/parameters	9018/0/496
Goodness-of-fit on F^2	1.070
Final R indexes [$I > 2\sigma(I)$]	$R1$ = 0.0420, $wR2$ = 0.1014
Largest diff. peak/hole /e Å^{-3}	2.544/–1.759

collection was performed using the COLLECT program,[53] integration and scaling of the reflections were performed with the HKL Denzo-Scalepack system of programs.[54] Absorption correction was carried out using the Gaussian method.[55] The structure was solved by direct methods and refined by full-matrix least-squares on F^2 by means of SHELX-97 package.[56] Hydrogen atoms were stereochemically positioned and refined with the riding model. Data collection and experimental details are summarized in Table 3.

The molecular and packing diagrams were generated using Ortep[57] and Mercury, respectively.[58] Puckering parameters were calculated using Platon for Windows.[59] Exact cone (θ°) and exact solid cone (Θ°) angles were computed using the Mathematica packages FindConeAngle[20] and FindSolidAngle,[22] respectively. The solid angles and G-parameters were calculated with Solid-G software.[23]

CCDC 1030349 (for **1**) contains the supplementary crystallographic data for this paper. These data can be obtained free of charge from The Cambridge Crystallographic Data Centre.

4.5. Biological activity

4.5.1. *Cell culture assay.* The title complex was assayed against human breast tumor cell line MDA-MB-231 (ATCC: HTB-26), DU-145, human prostate cancer cells (ATCC: HTB-81) and against the L929 cell line (ATCC: CCL-1). The cells MDAMB-231 and L929 routinely maintained in Dulbecco's modified Eagle's medium (DMEM) supplemented with 10 % fetal bovine serum (FBS); the DU-145 cells were maintained in RPMI-1640 supplemented with10 % FBS, at 37 °C in a humidified 5 % CO_2 atmosphere. After reaching confluence, the cells were detached by trypsinization and counted. For the cytotoxicity assay, 1.5×10^4 cells well^{-1} were seeded in 200 µL of complete medium in 96-well assay microplates. The plates were incubated at 37 °C in 5 % CO_2 for 24 h to allow cell adhesion. The tested compound was dissolved in sterile DMSO (stock solution with maximum concentration of 20 mmol L^{-1}) and diluted to 20, 10, 5, 0.25, 0.62, 0.15, 0.039 mmol L^{-1}.

From diluted compound 1µL aliquots were added to 200 µL medium giving a final concentration of approximately 0.5 % of DMSO and a final concentration of the complex diluted of about 100 times. Cells were exposed to the compound during a 48 h-period. Cell respiration, as an indicator of cell viability, was determined by the mitochondrial-dependent reduction of MTT [3-(4,5-dimethylthiazol-2-yl)-2,5-diphenyltetrazolium bromide] to formazan.[60] MTT solution (0.5 mg/mL) was added to cell culture and incubated for 3 h, after which 100 µL of 2-propanol was added to dissolve the precipitated formazan crystals. The conversion of MTT to formazan by metabolically viable cells was monitored in an automated microplate reader at 540 nm. The percent cell viability was calculated by dividing the average absorbance of the cells treated with the test compound by that of the control. The % cell viability was plotted against drug concentration (logarithmic scale) to determine the IC_{50} (drug concentration at which 50 % of the cells are viable in relation to the control), with the error estimated from the average of 3 trials.

4.5.2. *Anti-mycobacterial activity.* The anti-mycobacterium tuberculosis activity of the complex was determined by the REMA (resazurin microtiter assay) method.[61] Stock solutions of the tested compounds were prepared in DMSO and diluted in Middlebrook 7H9 broth (Difco) supplemented with oleic acid, albumin, dextrose and catalase (OADC), performed by Precision XS (Biotek®) to obtain the final drug concentration range of 0.09–25 µg mL^{-1}. Isoniazid was dissolved in distilled water and rifampicin in DMSO, and both were used as standard drugs. A suspension of MTB H37Rv ATCC 27294 was cultured in Middlebrook 7H9 broth supplemented with OADC and 0.05 % Tween 80.

The cultures were frozen at –80 °C in aliquots. After two days the CFU per mL (colony formation unit per mL) of an aliquot was determined. The concentrations were adjusted by 5×10^5 CFU per mL and 100 µL of the inoculum were added to each well of a 96-well microplate together with 100 µL of the compounds. Samples were set up in triplicate. The plates were incubated for 7 days at 37 °C. Resazurin (solubilized in water) was added (30 µL of 0.01 %). The

fluorescence of the wells was read after 24 h with a Cytation 3 (Biotek®). The MIC (minimum inhibitory concentration) was defined as the lowest concentration resulting in 90 % inhibition of MTB growth.

Disclosure statement

No potential conflict of interest has been reported by the authors.

Acknowledgments

This work was supported by CAPES (Project Oficio/CSS/CGCI/23038009487/2011-25/DRI/CAPES, AUX CAPES-MES-Cuba, 339/2011).

Keywords: Platinum · Phosphine ligands · Structure elucidation · Steric descriptors · Anagostic interactions · Biological activity

[1] R. Lesyk, B. Zimenkovsky, *Curr. Org. Chem.* **2004**, *8*, 1547.
[2] R. Lesyk, O. Vladzimirska, S. Holota, L. Zaprutko, A. Gzella, *Eur. J. Med. Chem.* **2007**, *42*, 641.
[3] D. Havrylyuk, B. Zimenkovsky, O. Vasylenko, L. Zaprutko, A. Gzella, R. Lesyk, *Eur. J. Med. Chem.* **2009**, *44*, 1396.
[4] M. Mushtaque, F. Avecilla, M. S. Khan, Z. B. Hafeez, M. M. A. Rezvi, A. Srivastava, *J. Mol. Struct.* **2017**, *1141*, 119.
[5] A. A. Alama, B. Tasso, F. Novelli, F. Sparatore, *Drug Discovery Today* **2009**, *14*, 500.
[6] A. M. Plutín, A. Álvarez, R. Mocelo, R. Ramos, E. E. Castellano, M. M. da Silva, L. Colina-Vegas, F. R. Pavan, A. A. Batista, *Inorg. Chem. Commun.* **2016**, *63*, 74.
[7] S. K. Seth, P. Manna, N. J. Singh, M. Mitra, A. D. Jana, A. Das, S. R. Choudhury, T. Kar, S. Mukhopadhyay, K. S. Kim, *CrystEngComm* **2013**, *15*, 1285.
[8] M. M. Habtu, S. A. Bourne, K. R. Koch, R. C. Luckay, *New J. Chem.* **2006**, *30*, 155.
[9] A. Saeed, M. Bolte, M. F. Erben, H. Pérez, *CrystEngComm* **2015**, *17*, 7551.
[10] a) N. Gunasekaran, N. Remya, S. Radhakrishnan, R. Karvembu, *J. Coord. Chem.* **2011**, *64*, 491; b) N. Gunasekaran, R. Karvembu, *Inorg. Chem. Commun.* **2010**, *13*, 952; c) N. Gunasekaran, P. Jerome, S. W. Ng, E. R. T. Tiekink, R. Karvembu, *J. Mol. Catal. A* **2012**, *353*, 156; d) N. Gunasekaran, P. Ramesh, M. N. G. Ponnuswamy, R. Karvembu, *Dalton Trans.* **2011**, *40*, 12519.
[11] a) S. J. Connon, *Chem. Commun.* **2008**, *22*, 2499; b) Y.-B. Huang, W.-B. Yi, C. Cai. *Fluorous chemistry*. In: Horváth, IT editor, Berlin: Springer, p. 191–212 (**2012**).
[12] a) A. Saeed, U. Flörke, M. F. Erben, *J. Sulfur Chem.* **2014**, *35*, 318; b) A. Saeed, R. Qamar, T. A. Fattah, U. Flörke, M. F. Erben, *Res. Chem. Intermed.* **2017**, *43*, 3053.
[13] M. L. Clarke & J. J. R. Frew. *Organometallic Chemistry*, vol. 35, p. 19, the Royal Society of Chemistry: London, (**2009**).
[14] a) M. Landman, T. Levell, P. H. van Rooyen, J. Conradie, *J. Mol. Struct.* **2014**, *1065*, 29; b) J. Flapper, P. Wormald, M. Lutz, A. L. Spek, P. W. N. M. van Leeuwen, C. J. Elsevier, P. C. J. Kamer, *Eur. J. Inorg. Chem.* **2008**, *31*, 4968.
[15] W. H. Hang, P. J. Dyson, *Eur. J. Inorg. Chem.* **2006**, 4003–4018.
[16] R. Sáez, J. Lorenzo, M. J. Prieto, M. Font-Bardia, T. Calvet, N. Omeñaca, M. Vilaseca, V. Moreno, *J. Inorg. Biochem.* **2014**, *136*, 1–12.
[17] L. Biancalana, S. Zacchini, N. Ferri, M. G. Lupo, G. Pampaloni, F. Marchetti, *Dalton Trans.* **2017**, *46*, 16589–16604.
[18] C. A. Tolman, *Chem. Rev.* **1977**, *77*, 313.
[19] a) G. Ferguson, P. J. Roberts, E. C. Alyea, M. Khan, *Inorg. Chem.* **1978**, *17*, 2965; b) T. L. Brown, K. J. Lee, *Coord. Chem. Rev.* **1993**, *128*, 89; c) T. E. Müller, D. M. P. Mingos, *Transit. Met. Chem.* **1995**, *20*, 533; d) K. A. Bunten, L. Chen, A. L. Fernández, A. J. Poë, *Coord. Chem. Rev.* **2002**, *233*, 41; e) S. Otto, *Acta Crystallogr., Sect. C* **2001**, *57*, 793.
[20] J. A. Bilbrey, A. H. Kazez, J. Locklin, W. D. Allen, *J. Comput. Chem.* **2013**, *34*, 1189.
[21] J. A. Bilbrey & W. D. Allen. *Ligand Steric Descriptors, Chapter one*, Annual Reports in Computational Chemistry, Vol. 9, Elsevier B. V. (**2013**).
[22] J. A. Bilbrey, A. H. Kazez, J. Locklin, W. D. Allen, *J. Chem. Theory Comput.* **2013**, *9*, 5734.
[23] I. A. Guzei, M. Wendt, *Dalton Trans.* **2006**, 3991.
[24] N. H. Huy, U. Abram, *Inorg. Chem.* **2007**, *46*, 5310.
[25] A. M. Plutín, R. Mocelo, A. Álvarez, R. Ramos, E. E. Castellano, M. R. Cominetti, A. E. Graminha, A. G. Ferreira, A. A. Batista, *J. Inorg. Biochem.* **2014**, *134*, 76.
[26] G. Kemp, A. Roodt, W. Purcell, K. R. Koch, *J. Chem. Soc., Dalton Trans.* **1997**, 4481.
[27] a) A. Saeed, Z. Ashraf, M. F. Erben, J. Simpson, *J. Mol. Struct.* **2017**, *1129*, 283; b) A. A. Batista, K. Wonrath, S. L. Queiroz, O. M. Porcu, E. E. Castellano, C. Barberato, *Trans. Met. Chem.* **2001**, *26*, 365.
[28] K. Nakamoto. *Infrared and Raman Spectra of Inorganic and Coordination Compounds*, 4th ed; John Wiley & Sons: New York (**1986**).
[29] A. Pérez-Rebolledo, O. E. Piro, E. E. Castellano, L. R. Teixeira, A. A. Batista, H. Beraldo, *J. Mol. Struct.* **2006**, *794*, 18.
[30] a) B. H. Abdullah, Y. M. Salh, *Orient. J. Chem.* **2010**, *26*, 763; b) A. Saeed, S. Ashraf, J. M. White, D. B. Soria, C. A. Franca, M. F. Erben, *Spectrochim. Acta* **2015**, *150A*, 409.
[31] K. Koch, *Coord. Chem. Rev.* **2001**, *47*, 216.
[32] a) R. S. Correa, K. M. de Oliveira, F. G. Delolo, R. A. Mocelo, A. M. Plutín, M. R. Cominetti, E. E. Castellano, A. A. Batista, *J. Inorg. Biochem.* **2015**, *150*, 63; b) R. R. Cairo, A. M. Plutín, T. D. de Oliveira, A. A. Batista, E. E. Castellano, J. Duque, D. B. Soria, A. C. Fantoni, R. S. Corrêa, M. F. Erben, *Spectrochim. Acta* **2017**, *176A*, 8–17.
[33] S. Ahmad, A. A. Isab, S. Ali, *Trans. Met. Chem.* **2006**, *31*, 1003.
[34] S. Ahmad, *Chem. Biodiversity* **2010**, *7*, 543.
[35] W. Villarreal, L. Colina-Vegas, C. R. de Oliveira, J. C. Tenorio, J. Ellena, F. C. Gozzo, M. R. Cominetti, A. G. Ferreira, M. A. B. Ferreira, M. Navarro, A. A. Batista, *Inorg. Chem.* **2015**, *54*, 11709.
[36] W. J. Geary, *Coord. Chem. Rev.* **1971**, *7*, 81.
[37] M. Kampf, R. Richter, S. Gerber, R. Kirmse, *Z. Anorg. Allg. Chem.* **2004**, *630*, 1437.
[38] L. Yang, D. R. Powell, R. P. Houser, *Dalton Trans.* **2007**, 955.
[39] M. H. Johansson, S. Otto, *Acta Crystallogr., Sect. C* **2000**, *56*, e12–e15.
[40] T. Niksch, H. Görls, W. Weigand, *Eur. J. Inorg. Chem.* **2010**, 95–105.
[41] D. Cremer, J. A. Pople, *J. Am. Chem. Soc.* **1975**, *97*, 1354.
[42] a) C. Janiak, S. Temizdemir, S. Dechert, W. Deck, F. Girgsdies, J. Heinze, M. J. Kolm, T. G. Scharmann, O. M. Zipffel, *Eur. J. Inorg. Chem.* **2000**, 1229; b) C. Janiak, *J. Chem. Soc., Dalton Trans.* **2000**, 3885.
[43] a) M. Brookhart, M. L. H. Green, *J. Organomet. Chem.* **1983**, *250*, 395; b) M. Brookhart, M. L. H. Green, G. Parkin, *Proc. Natl. Acad. Sci. USA* **2007**, *104*, 6908.
[44] N. Singh, B. Singh, K. Thapliyal, M. G. B. Drew, *Inorg. Chim. Acta* **2010**, *363*, 3589.
[45] M. G. Derry Holaday, G. Tarafdar, A. Kumar, M. L. P. Reddy, A. Srinivasan, *Dalton Trans.* **2014**, *43*, 7699.
[46] a) L. Brammer, *Dalton Trans.* **2003**, 3145; b) J. C. Lewis, J. Wu, R. G. Bergman, J. A. Ellman, *Organometallics* **2005**, *24*, 5737.
[47] H. V. Huynh, L. R. Wong, P. S. Ng, *Organometallics* **2008**, *27*, 2231.
[48] A. Husain, S. A. A. Nami, S. P. Singh, M. Oves, K. S. Siddiqi, *Polyhedron* **2011**, *30*, 33.
[49] R. J. H. Clark, C. D. Flint, A. J. Hempleman, *Spectrochim. Acta* **1987**, *43A*, 805.
[50] M. A. Rodrigues, I. M. Marzano, G. H. Ribeiro, L. Colina-Vegas, M. Pivatto, A. P. S. Fontes, C. M. Ribeiro, F. R. Pavan, K. J. de Almeida, A. A. Batista, E. C. Pereira-Maia, W. Guerra, *Polyhedron* **2015**, *98*, 146.
[51] A. M. Plutín, A. Alvarez, R. Mocelo, R. Ramos, O. C. Sánchez, E. E. Castellano, M. M. da Silva, W. Villarreal, L. Colina-Vegas, F. R. Pavan, A. A. Batista, *J. Braz. Chem. Soc.* **2018**, *29*, 1.
[52] A. M. Plutín, H. Márquez, M. Morales, M. Sosa, L. Morán, Y. Rodríguez, M. Suárez, C. Seoane, N. Martín, *Tetrahedron* **2000**, *56*, 1533.
[53] Enraf-Nonius; COLLECT, Nonius BV: Delft, the Netherlands (1997–2000).
[54] Z. Otwinowski, W. Minor. In: Methods in Enzymology, Vol. 276, p. 307–326 (Eds.: C. W. Carter Jr., R. M. Sweet); *Academic Press*: New York (**1997**).
[55] R. H. Blessing, *Acta Crystallogr., Sect. A* **1995**, *51*, 33.
[56] G. M. Sheldrick, *Acta Crystallogr., Sect. A* **2008**, *64*, 112–122.
[57] L. J. Farrugia, *J. Appl. Crystallogr.* **2012**, *45*, 849.

[58] C. F. Macrae, I. J. Bruno, J. A. Chisholm, P. R. Edgington, P. McCabe, E. Pidcock, L. Rodriguez Monge, R. Taylor, J. van de Streek, A. Wood, *J. Appl. Crystallogr.* **2008**, *41*, 466.
[59] A. Spek, *Acta Crystallogr., Sect. D* **2009**, *65*, 148.
[60] T. Mosmann, *J. Immunol. Methods* **1983**, *65*, 55.
[61] J. C. Palomino, A. Martin, M. Camacho, H. Guerra, J. Swings, F. Portaels, *Antimicrob. Agents Chemother.* **2002**, *46*, 2720.

Received: January 10, 2019

